BIOMOLECULES & THERAPEUTICS

Original Article
Biomol Ther 23(4), 357-366 (2015)

Isorhamnetin Protects Human Keratinocytes against Ultraviolet B-Induced Cell Damage

Xia Han[1], Mei Jing Piao[1], Ki Cheon Kim[1], Susara Ruwan Kumara Madduma Hewage[1], Eun Sook Yoo[1], Young Sang Koh[1], Hee Kyoung Kang[1], Jennifer H Shin[2], Yeunsoo Park[3], Suk Jae Yoo[3], Sungwook Chae[4] and Jin Won Hyun[1,*]

[1]School of Medicine, Jeju National University, Jeju 690-756, [2]Department of Mechanical Engineering & Graduate School of Medical Science and Engineering, KAIST, Daejeon 305-701, [3]National Fusion Research Institute, Plasma Technology Research Center, Gunsan 573-540, [4]Aging Research Center, Korea Institute of Oriental Medicine, Daejeon 305-811, Republic of Korea

Abstract

Isorhamnetin (3-methylquercetin) is a flavonoid derived from the fruits of certain medicinal plants. This study investigated the photoprotective properties of isorhamnetin against cell damage and apoptosis resulting from excessive ultraviolet (UV) B exposure in human HaCaT keratinocytes. Isorhamnetin eliminated UVB-induced intracellular reactive oxygen species (ROS) and attenuated the oxidative modification of DNA, lipids, and proteins in response to UVB radiation. Moreover, isorhamnetin repressed UVB-facilitated programmed cell death in the keratinocytes, as evidenced by a reduction in apoptotic body formation, and nuclear fragmentation. Additionally, isorhamnetin suppressed the ability of UVB light to trigger mitochondrial dysfunction. Taken together, these results indicate that isorhamnetin has the potential to protect human keratinocytes against UVB-induced cell damage and death.

Key Words: Isorhamnetin, Ultraviolet B, Reactive oxygen species, Human keratinocyte, Programmed cell death

INTRODUCTION

Excessive or chronic ultraviolet (UV) radiation induces many types of skin damage, including sunburn, photoaging, corneal injury, and inflammation; extreme UV exposure can even compromise the immune system (Matsumura and Ananthaswamy, 2004; Liu *et al*., 2012). UV radiation consists of three kinds of energy: UVA (~320-540 nm), UVB (~280-320 nm), and UVC (~100-320 nm) light. While UVA and UVB light both provoke skin damage, the latter is stronger than the former and accordingly, is associated with graver biological insults.

UVB radiation is mostly absorbed in the epidermis, where it mainly affects epidermal cells, especially keratinocytes (Zeng *et al*., 2014). However, ~10-30% of UVB energy can reach the upper dermis, and hence, UVB light is also hazardous to fibroblasts and the extracellular matrix (Everett *et al*., 1966; Rosette and Karin, 1996). Additionally, UVB light interacts with intracellular chromophores and photosensitizers to engender severe oxidative stress in skin cells, together with transient as well as permanent genetic damage. At a more fundamental level, these oxidative reactions activate cytoplasmic signal transduction pathways associated with cell growth, differentiation, and senescence, and ultimately, connective tissue degradation (Helenius *et al*., 1999).

UVB radiation triggers two predominant types of cytotoxic damage to the skin that interfere with normal cellular functions, and finally culminate in photodamage, photoaging, and photocarcinogenesis (Sander *et al*., 2004). First, UVB light directly damages DNA via the formation of thymine-thymine cyclobutane dimers (Budden and Bowden, 2013). Second, UVB light indirectly damages DNA, lipids and proteins via generation of unwarranted levels of reactive oxygen species (ROS) (Wäster and Ollinger, 2009; Lee *et al*., 2013). Although the skin has efficient antioxidant defense mechanisms against a variety of endogenous and exogenous insults (Lyu and Park, 2012), an overabundance of UVB-induced ROS disrupts this defensive capacity and precipitates irrevocable oxidative injury (Scandalios, 2002).

Natural antioxidants have received ample attention as prospective preventative or curative agents against skin disease and damage caused by long-term or extreme exposure to UVB (Afaq, 2011; Yin *et al*., 2013). For example, isorhamnetin

Open Access **http://dx.doi.org/10.4062/biomolther.2015.005**

Received Jan 9, 2015 **Revised** Jan 29, 2015 **Accepted** Feb 26, 2015
Published online Jul 1, 2015

***Corresponding Author**
E-mail: jinwonh@jejunu.ac.kr
Tel: +82-64-754-3838, Fax: +82-64-702-2687

is an antioxidant flavonoid derived from the fruits of certain medicinal plants, including *Hippophae rhamnoides* L. (Li *et al*., 2014; Yang *et al*., 2014). Nevertheless, the photoprotective role of isorhamnetin against UVB-provoked skin damage remains unknown. Accordingly, this study examined the ability of isorhamnetin to safeguard cultured human keratinocytes from injury resulting from UVB exposure.

MATERIALS AND METHODS

Reagents

Isorhamnetin (3,5,7-trihydroxy-2-(4-hydroxy-3-methoxyphenyl)-4-benzopyrone, purity: ≥98%) was purchased from Santa Cruz Biotechnology Co. (Santa Cruz, CA, USA) and dissolved in dimethylsulfoxide (DMSO). The ultimate density of DMSO did not exceed 0.02% in any of the experiments. N-acetyl cysteine (NAC), [3-(4,5-dimethylthiazol-2-yl)-2,5-diphenyltetrazolium] bromide (MTT), 2',7'-dichlorodihydrofluorescein diacetate (DCF-DA), Hoechst 33342 dye, and 5,5-dimethyl-1-pyrroline-N-oxide (DMPO) were purchased from Sigma Chemical Co. (St. Louis, MO, USA), while 5,5',6,6'-tetrachloro-1,1',3,3'-tetraethyl-benzimidazolylcarbocyanine iodide (JC-1) was purchased from Invitrogen (Carlsbad, CA, USA). Diphenyl-1-pyrenylphosphine (DPPP) was purchased from Molecular Probes (Eugene, OR, USA). All other chemicals and reagents were of analytical grade.

Cell culture

The human keratinocyte HaCaT cell line was supplied by Amore Pacific Co. (Yongin, Republic of Korea). Cells were incubated in a 5% CO_2/95% atmosphere at 37°C in RPMI 1640 medium (Invitrogen) containing 10% heat-inactivated fetal calf serum, streptomycin (100 μg/ml), and penicillin (100 units/ml).

Cell viability assay

The potential cytotoxicity of isorhamnetin against HaCaT keratinocytes was investigated by using the colorimetric MTT assay, which is based on the reduction of a tetrazolium salt by mitochondrial dehydrogenases in viable cells. Cells were seeded into 24-well plates at a density of 1.0×10^5 cells/well. Sixteen hours later, they were pretreated with isorhamnetin at concentrations of 0, 2.5, 5, 10, and 20 μM.

The photoprotective actions of isorhamnetin against UVB radiation were next assessed in HaCaT keratinocytes. Cells were pretreated with isorhamnetin (5 μM) for 1 h, exposed to UVB light at a dose of 30 mJ/cm^2, and then incubated at 37°C for additional 24 h. MTT stock solution (50 μl; 2 mg/ml) was added to each well to yield a total reaction volume of 200 μl. After incubation for 4 h, the medium was aspirated. The formazan crystals in each well were dissolved in DMSO (150 μl), and the absorbance at 540 nm was read on a scanning multi-well spectrophotometer (Carmichael *et al*., 1987).

Detection of intracellular ROS

To measure intracellular ROS content in UVB-irradiated HaCaT keratinocytes, cells were seeded into 24-well plates at a density of 1.0×10^5 cells/well. Sixteen hours later, the cells were pretreated for 1 h at 37°C with 1 mM NAC, a powerful antioxidant used as the positive control, or with 5 μM isorhamnetin. Next, the cells were exposed to UVB radiation (30 mJ/cm^2). Two hours later, the cells were loaded with DCF-DA solution (50 μM) and incubated for 30 min at 37°C. The fluorescence of the 2',7'-dichlorofluorescein (DCF) product was detected and quantitated by using a LS-5B spectrofluorometer (PerkinElmer, Waltham, MA, USA).

Additionally, the ROS scavenging potential of isorhamnetin was evaluated in UVB-irradiated cells via flow cytometry. Cells were seeded at a density of 1.0×10^5 cells/well. Sixteen hours after plating, they were pretreated with 5 μM isorhamnetin for 1 h, exposed to UVB light, and incubated for an additional 9 h at 37°C. Cells were then loaded with DCF-DA (40 μM) and incubated for 30 min at 37°C. The fluorescence of the DCF product was detected via flow cytometry by using a FACSCalibur instrument (Becton Dickinson, Mountain View, CA, USA) (Rosenkranz *et al*., 1992).

Lastly, image analysis of intracellular ROS was conducted by seeding the keratinocytes onto four-well chamber slides at a density of 1.0×10^5 cells/ml. Sixteen hours after plating, the cells were pretreated with 5 μM isorhamnetin for 1 h, and then irradiated with UVB light. After an additional 24 h, 40 μM DCF-DA was added to each well, and the samples were incubated for another 30 min at 37°C. The stained cells were then washed with PBS and mounted onto a chamber slide in mounting medium (Dako, Carpentaria, CA, USA). Images of the cultures were captured by using an LSM 5 PASCAL laser scanning confocal microscope and the accompanying LSM 5 PASCAL software (Carl Zeiss, Jena, Germany).

Superoxide anion and hydroxyl radical detection by electron spin resonance (ESR) spectrometry

The xanthine/xanthine oxidase system was employed to generate the superoxide anion, and the generated superoxide anion was reacted with the nitrone spin trap, DMPO. The resultant DMPO/•OOH adducts were detected by using a JES-FA ESR spectrometer (JEOL, Ltd., Tokyo, Japan), as previously described (Ueno *et al*., 1984; Kohno *et al*., 1994). Briefly, isorhamnetin (20 μl; 5 μM) was mixed with xanthine oxidase (0.25 U), xanthine (10 mM), and DMPO (3 M), and ESR signaling was recorded at 2.5 min after reaction occurrence. The ESR spectrometry parameters were set as follows: center field=336 mT, power=1.00 mW, modulation width=0.2 mT, sweep time=30 sec, sweep width=10 mT, time constant=0.03 sec, and temperature=25°C.

Next, the Fenton reaction (H_2O_2+$FeSO_4$) was employed to generate the hydroxyl radical, and the generated hydroxyl radical was reacted with DMPO. The resultant DMPO/•OH adducts were detected by using an ESR spectrometer, as previously described (Li *et al*., 2004). The ESR spectrum was recorded at 2.5 min after isorhamnetin (20 μl; 5 μM) was mixed with $FeSO_4$ (10 mM), H_2O_2 (10 mM), and DMPO (0.3 M). The ESR spectrometry parameters were set as indicated above for superoxide anion detection.

Nuclear staining with Hoechst 33342 dye

HaCaT keratinocytes were pretreated with 5 μM isorhamnetin or 1 mM NAC for 1 h, followed by exposure to UVB light. After an additional incubation for 24 h at 37°C, the DNA-specific fluorescent dye, Hoechst 33342 (20 μM), was added to each well, and the keratinocytes were incubated for another 10 min at 37°C. The stained cells were visualized by using a fluorescence microscope equipped with a CoolSNAP-Pro color digital camera. The degree of nuclear condensation was evaluated, and apoptotic cells were counted.

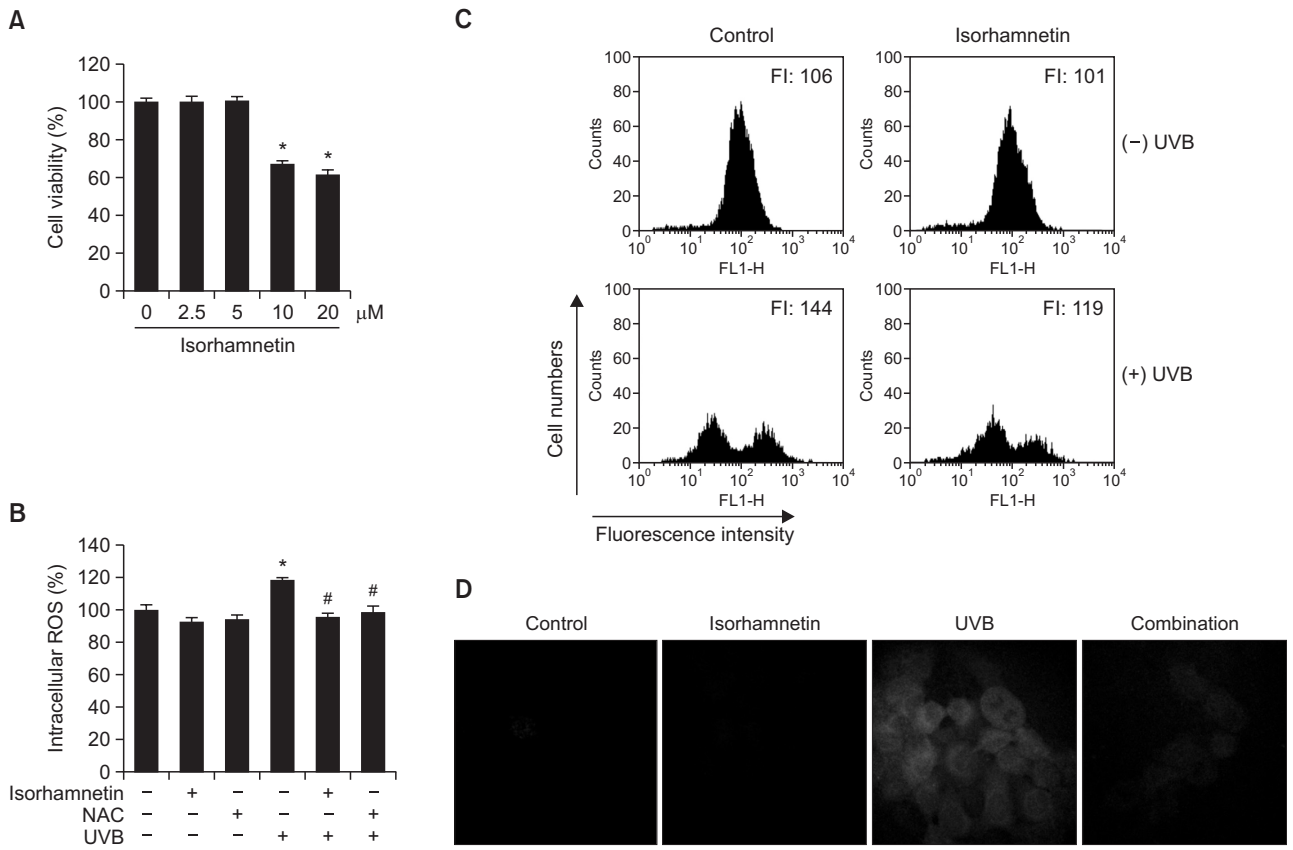

Fig. 1. Isorhamnetin scavenges ROS. (A) HaCaT keratinocytes were pretreated with isorhamnetin at various concentrations. After incubation for 24 h, cell viability was assessed by using the MTT assay. Cell viability is expressed in each case as a percentage of the untreated control (100%). (B-D) Cells were treated with 5 μM isorhamnetin for 1 h or (B) 1 mM NAC for 1 h, and then exposed to UVB light. After incubation for 30 min, intracellular ROS levels were detected by using (B) fluorescence spectrofluorometry, (C) flow cytometry, and (D) confocal microscopy after DCF-DA staining. *Significantly different from control (p<0.05); #significantly different from UVB-irradiated cells (p<0.05). FI, fluorescence intensity. Combination, isorhamnetin+UVB light. (E) The superoxide anion generated by the xanthine/xanthine oxidase (XO) system was reacted with, and the resulting •OOH adducts were detected by ESR spectrometry. The results are expressed as representative peak data and histograms. Control: PBS; isorhamnetin: isorhamnetin+PBS; superoxide anion: PBS+xanthine+xanthine oxidase; isorhamnetin+superoxide anion: isorhamnetin+xanthine+xanthine oxidase. (F) The hydroxyl radical generated by the Fenton reaction (H_2O_2+$FeSO_4$) was reacted with and the resulting •OH adducts were detected by ESR spectrometry. Results are expressed as representative peak data and histograms. Control: PBS; isorhamnetin: isorhamnetin+PBS; hydroxyl radical: PBS+$FeSO_4$+H_2O_2; isorhamnetin+hydroxyl radical: isorhamnetin+$FeSO_4$+H_2O_2.

Detection of sub G_1 hypodiploid cells

Propidium iodide staining-based flow cytometry was performed to evaluate the fraction of apoptotic sub G_1 cells with hypodiploid DNA content. Cells were pretreated with 5 μM isorhamnetin for 1 h, exposed to UVB radiation, and harvested 24 h later. The isorhamnetin-pretreated, irradiated cells were fixed with 70% ethanol (1 ml) for 30 min at 4°C, washed twice with PBS, and incubated in the dark for 30 min at 37°C in PBS containing PI and RNase A. Flow-cytometric analysis was performed by using a FACSCalibur instrument. The percentage of sub G_1 hypodiploid cells was assessed based on histograms generated by CellQuest and ModFit Software (Becton Dickinson).

Terminal deoxynucleotidyl transferase-mediated digoxigenin-dUTP nick end labeling (TUNEL) assay

The TUNEL assay was performed by using an *in situ* cell death detection kit (Roche Diagnostics, Mannheim, Germany) according to the manufacturer's instructions. This assay allows the detection of DNA fragmentation by labeling the terminal end of nucleic acids. Briefly, HaCaT keratinocytes were seeded onto chamber slides at a density of 1.0×10^5 cells/well. Twenty hours later, the cells were pretreated with isorhamnetin (5 μM) for 1 h, exposed to UVB radiation, and incubated for an additional 24 h. Cells were then fixed with 4% paraformaldehyde for 30 min at room temperature, permeabilized with 0.2% Triton X-100 for 2 min, washed with PBS, and incubated with the TUNEL reaction mixture for 1 h at 37°C. After washing again with PBS, the stained cells were mounted onto a microscope slide in mounting medium. Images of the cells were captured and quantified by using an Olympus IX 70 fluorescence microscope (Olympus Optical Co., Tokyo, Japan).

Detection of mitochondrial membrane potential ($\Delta\psi_m$)

HaCaT keratinocytes were seeded into 24-well plates at a density of 1.0×10^5 cells/well. Sixteen hours after plating, the cells were pretreated with 5 μM isorhamnetin for 1 h, exposed to UVB radiation, and then incubated for an additional 24 h at 37°C. The $\Delta\psi_m$ was analyzed by using MitoPT™ JC-1 reagent,

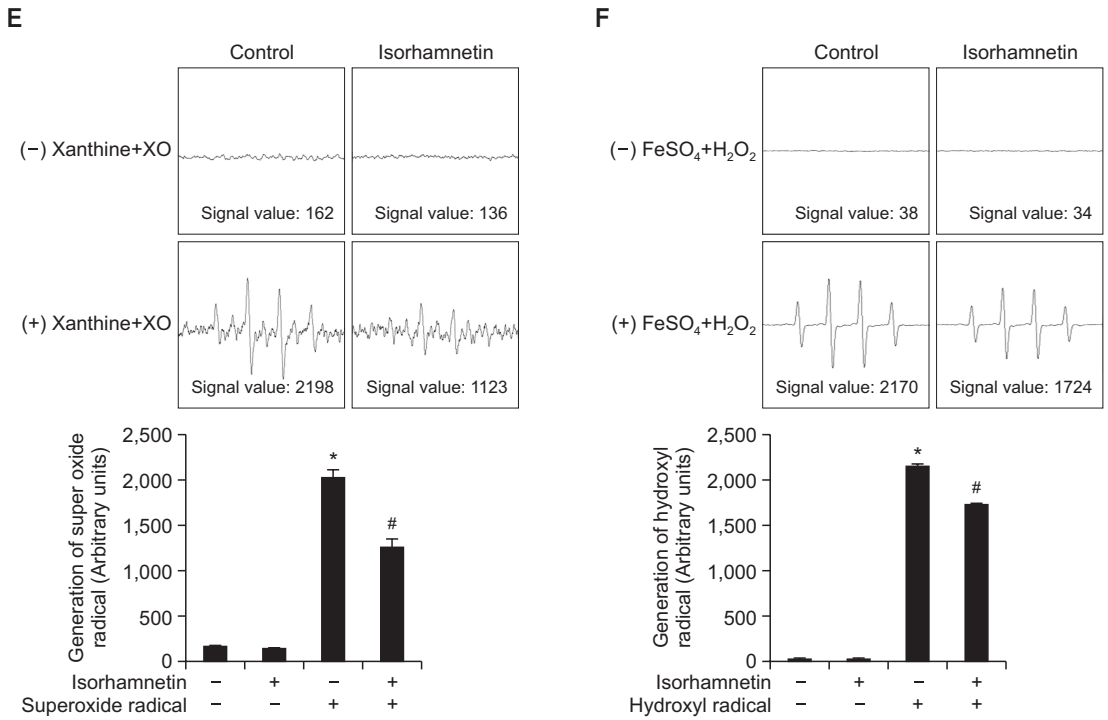

Fig. 1. Continued.

a lipophilic cationic fluorescent dye that easily penetrates cell and mitochondrial lipid bilayer membrane barriers. Once inside a healthy polarized mitochondrion, JC-1 redistributes itself within the organelle until a saturation level is reached, at which time J-aggregate formation occurs. This precipitated or aggregated form of JC-1 emits orange-red fluorescence upon excitation with blue light (488 nm). However, when the mitochondrial membrane potential collapses in apoptotic or metabolically stressed cells, JC-1 disperses throughout the cell in monomeric form. In the monomeric form, JC-1 emits green fluorescence upon excitation at 488 nm. After addition of 5 μM JC-1 and incubation for 30 min at 37°C (Cossarizza *et al*., 1993), the $\Delta\psi_m$ was analyzed in HaCaT keratinocytes via flow cytometry by using a FACSCalibur instrument.

Single-cell gel electrophoresis (comet assay)

Oxidative DNA strand breakage was detected via the comet assay, also known as single-cell gel electrophoresis (Singh, 2000; Rajagopalan *et al*., 2003). Twelve hours after isorhamnetin pretreatment and UVB radiation, a suspension of HaCaT keratinocytes was mixed with 75 μl of 0.5% low melting temperature agarose at 39°C, and the mixture was spread on a fully frosted microscopic slide pre-coated with 200 μl of 1% normal melting temperature agarose. The agarose was allowed to solidify, and the slide was covered with another 75 μl of 0.5% low melting temperature agarose, and then immersed in a lysis solution (2.5 M NaCl, 100 mM Na-EDTA, 10 mM Tris, 1% Trion X-100, and 10% DMSO, pH 10) at 4°C for 90 min. Next, the slides were placed in a gel electrophoresis apparatus containing 300 mM NaOH and 10 mM Na-EDTA, pH 13 for 40 min to allow for DNA unwinding and the expression of alkali-labile damage. An electrical field was then applied (300 mA, 25 V) for 20 min at room temperature to draw the negatively charged DNA towards the anode. After washing with a neutralizing buffer (0.4 M Tris, pH 7.5) for 5 min at 4°C, the slides were incubated with 40 μl of ethidium bromide and observed under a fluorescence microscope equipped with a Komet 5.5 image analyzing system (Kinetic Imaging, Ltd., Nottingham, UK). Percentages of total cellular fluorescence in the comet tails and the tail lengths were recorded from 50 cells per slide.

Lipid peroxidation assay

Oxidation damage to lipids was assessed by measuring levels of 8-isoprostane, an indicator of lipid peroxidation, secreted into the conditioned medium of irradiated HaCaT keratinocytes via colorimetric determination (Beauchamp *et al*., 2002). A commercial enzyme-linked immunosorbent assay kit (Cayman Chemical, Ann Arbor, MI, USA) was used to detect 8-isoprostane. Lipid peroxidation was also detected by using DPPP as a probe (Okimoto *et al*., 2000). DPPP is oxidized by lipid hydroperoxides to yield a fluorescent product, DPPP oxide, thereby providing an indication of oxidative membrane damage. HaCaT keratinocytes were pretreated with 5 μM isorhamnetin for 1 h, followed by exposure to UVB radiation. Six hours later, the cells were incubated with 20 μM DPPP for 30 min in the dark. Images of DPPP oxide fluorescence were captured by using a Zeiss Axiovert 200 inverted microscope at an excitation wavelength of 351 nm and an emission wavelength of 380 nm, and the intensity of the fluorescence was quantitated.

Protein carbonyl formation

Cells were pretreated with 5 μM isorhamnetin for 1 h, exposed to UVB radiation, and incubated for another 24 h. The

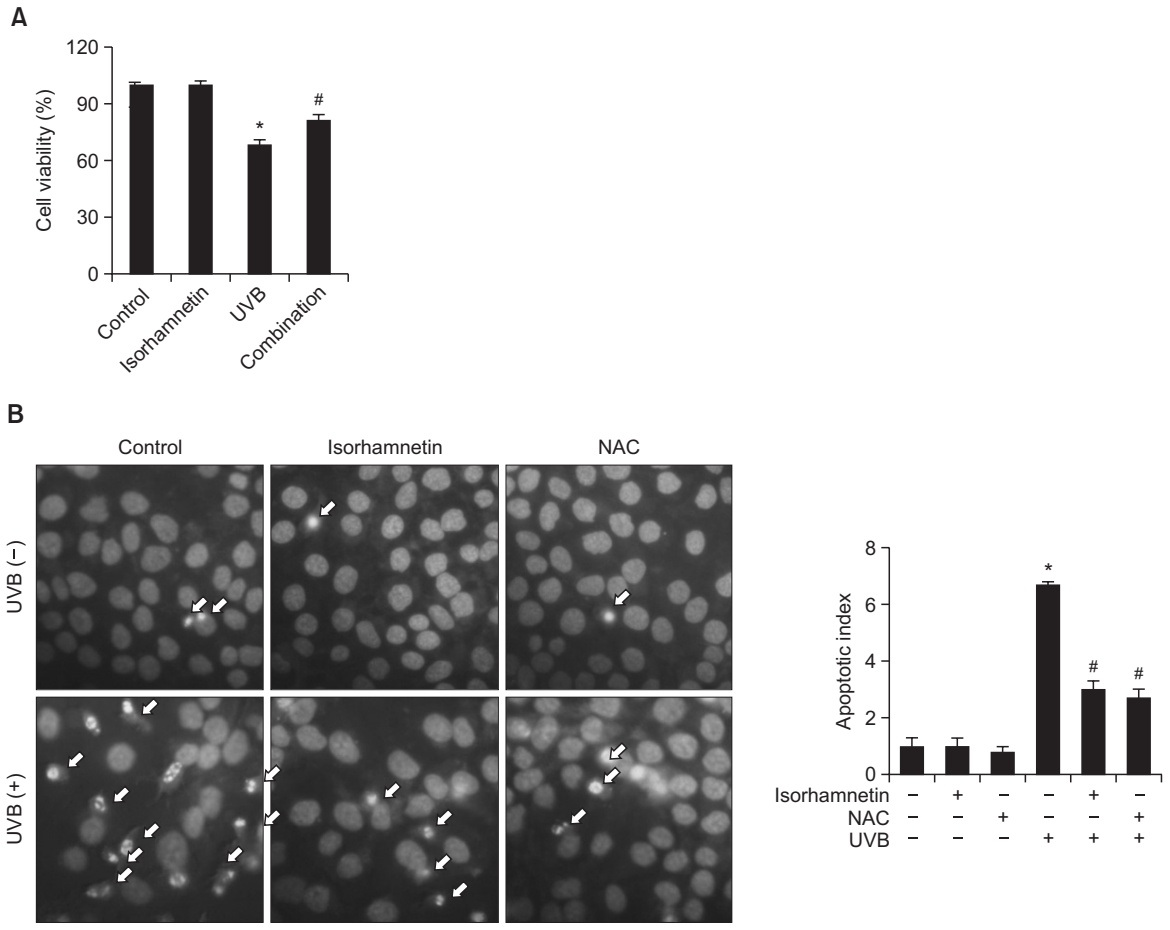

Fig. 2. Isorhamnetin ameliorates UVB-induced apoptosis. (A) HaCaT keratinocytes were pretreated with 5 μM isorhamnetin, exposed to UVB light 1 h later, and incubated for another 24 h. Cell viability was then determined by using the MTT assay. Cell viability is expressed in each case as a percentage of the untreated control (100%). (B) Cells were stained with Hoechst 33342 dye, and apoptotic bodies (arrows) were observed by fluorescence microscopy and quantitated. (C) Cells with apoptotic sub G1 DNA content were detected by flow cytometry after propidium iodide staining. (D) Apoptotic cells were detected by the TUNEL assay and quantitated. The arrows indicate TUNEL-positive cells. *Significantly different from control (p<0.05); #significantly different from UVB-irradiated cells (p<0.05). Combination, isorhamnetin+UVB light.

extent of protein carbonyl formation was determined by using an Oxiselect™ protein carbonyl enzyme-linked immunosorbent assay kit (Cell Biolabs, San Diego, CA, USA).

Statistical analysis

All measurements were performed in triplicate, and all values are expressed as the means ± the standard error of the mean. The results were subjected to an analysis of variance (ANOVA) and Tukey's post-hoc test to analyze differences between means. In each case, a p-value of < 0.05 was considered statistically significant.

RESULTS

Isorhamnetin attenuates UVB-induced ROS in HaCaT keratinocytes and scavenges free radicals in cell-free systems

We first performed a MTT assay to determine whether isorhamnetin by itself impacts the viability of HaCaT keratinocytes. Isorhamnetin alone exerted no cytotoxic actions against the keratinocytes at concentrations up to 5 μM, although the agent did show strong cytotoxicity at 10 and 20 μM (Fig. 1A). Therefore, 5 μM isorhamnetin was chosen as the optimal concentration for further experimentation.

We next measured intracellular ROS levels in HaCaT keratinocytes under various experimental conditions by using the oxidation-sensitive fluorescent dye, DCF-DA. UVB-irradiated cells showed significantly higher ROS content relative to untreated control cells. However, isorhamnetin pretreatment (5 μM) significantly decreased ROS levels in UVB-irradiated cells and was as efficacious as NAC, a well-known ROS scavenger used as the positive control (Fig. 1B). Intracellular ROS levels were also detected via flow cytometry after DCF-DA staining to assess the ROS scavenging capacity of isorhamnetin in UVB-irradiated cells. The fluorescence intensity levels in untreated control and isorhamnetin-pretreated cells were 106 and 101 arbitrary units, respectively, signifying that isorhamnetin by itself does not generate intracellular ROS. However, the compound substantially inhibited ROS accumulation in UVB-exposed cells (fluorescence intensity=144 and 119 for

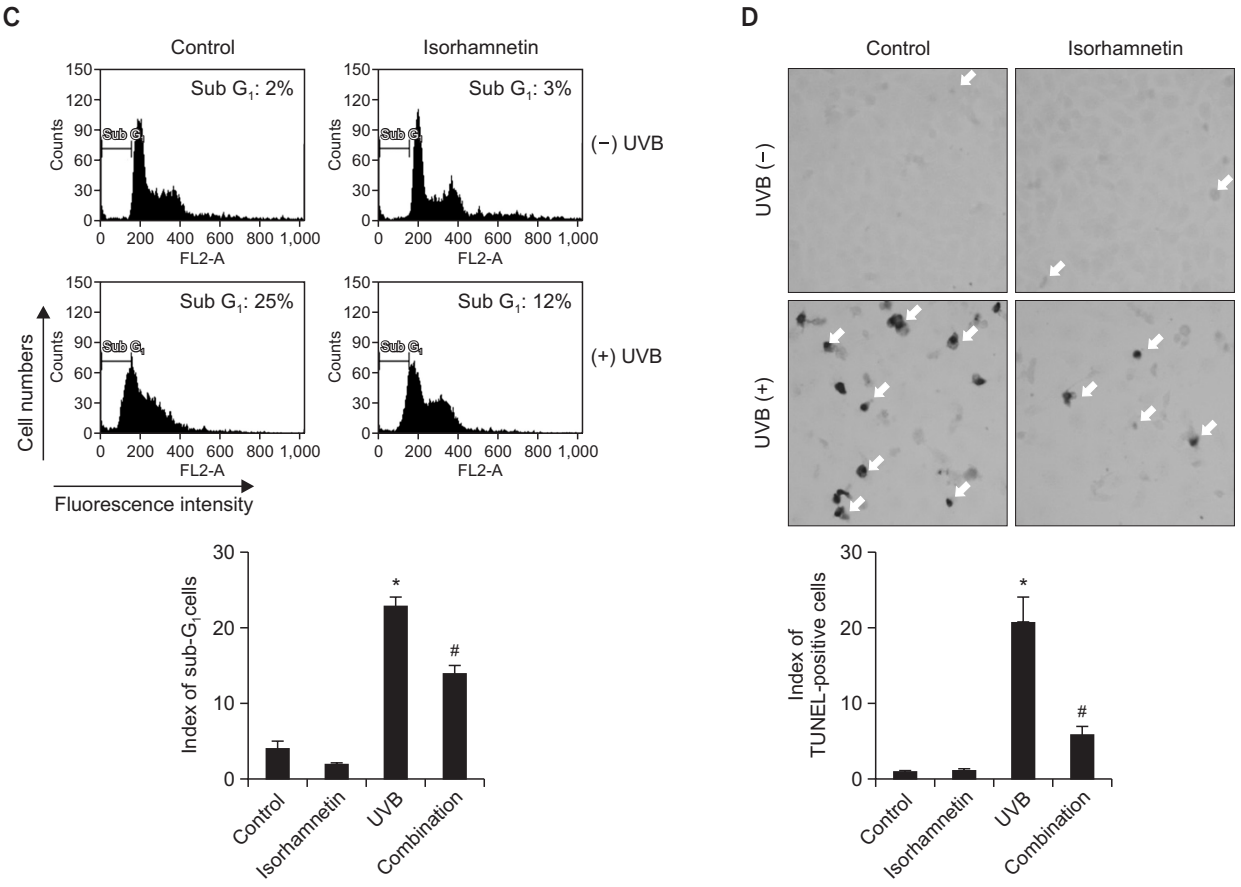

Fig. 2. Continued.

UVB-irradiated vs. UVB-/ isorhamnetin-treated cells, respectively; Fig. 1C). Moreover, confocal microscopy confirmed the flow cytometry findings, showing elevated ROS fluorescence in UVB-irradiated vs. UVB-irradiated/isorhamnetin-pretreated cells (Fig. 1D). Altogether, the results of Figure 1B-D indicate that isorhamnetin scavenges intracellular ROS induced by UVB exposure.

The scavenging effects of isorhamnetin against the superoxide anion and the hydroxyl radical were also explored in cell-free systems by ESR spectrometry. The superoxide anion signal in the xanthine/xanthine oxidase system increased from 162 in the control sample and 136 in the isorhamnetin-alone sample to 2198 in the xanthine/xanthine oxidase sample; however, the addition of isorhamnetin to the xanthine/xanthine oxidase sample significantly decreased the superoxide anion signal to 1123 (Fig. 1E). Similar results were found in the Fenton reaction system, where the hydroxyl radical signal increased from 38 in the control sample and 34 in the isorhamnetin-alone sample to 2170 in the Fenton reaction sample, but the addition of isorhamnetin to the Fenton reaction sample significantly decreased the hydroxyl radical signal to 1724 (Fig. 1F).

Isorhamnetin protects HaCaT keratinocytes against UVB-induced apoptosis

UVB radiation is well-known for its capacity to aggravate apoptosis in human keratinocytes (Schwarz *et al*., 1995). Therefore, the ability of isorhamnetin to improve cell survival in UVB-irradiated HaCaT keratinocytes was next investigated. Cell viability was significantly reduced in UVB-exposed vs. untreated control cells. Nevertheless, isorhamnetin pretreatment significantly overturned the effects of UVB light, with 81% vs. 69% cell viability observed in UVB-irradiated/isorhamnetin-pretreated vs. UVB-irradiated cultures (Fig. 2A).

Dynamic changes in nuclear chromatin compaction are characteristic of apoptotic execution (Wyllie *et al*., 1984). Therefore, HaCaT keratinocyte nuclei were stained with Hoechst 33342 dye to visualize nuclear fragmentation via fluorescence microscopy. Obvious nuclear fragmentation occurred in UVB-irradiated cells (apoptotic index=6.7), but the nuclear fragmentation rate was dramatically reduced by pretreatment with isorhamnetin (apoptotic index=3.0; compare with 2.7 for the positive control, NAC) (Fig. 2B).

The cytoprotective effects of isorhamnetin pretreatment against UVB-induced apoptosis were additionally confirmed by determination of the fraction of the cell population with apoptotic sub G_1 DNA content. The percentage of cells with apoptotic sub G_1 DNA content increased from 3% and 2% in untreated control and isorhamnetin-pretreated cells, respectively, to 25% in UVB-irradiated cells. Nonetheless, pretreatment with isorhamnetin significantly decreased this value to 12% (Fig. 2C). Moreover, the high level of DNA fragmentation in UVB-irradiated cells was significantly overturned by isorhamnetin pretreatment, as assessed by the TUNEL assay (Fig. 2D).

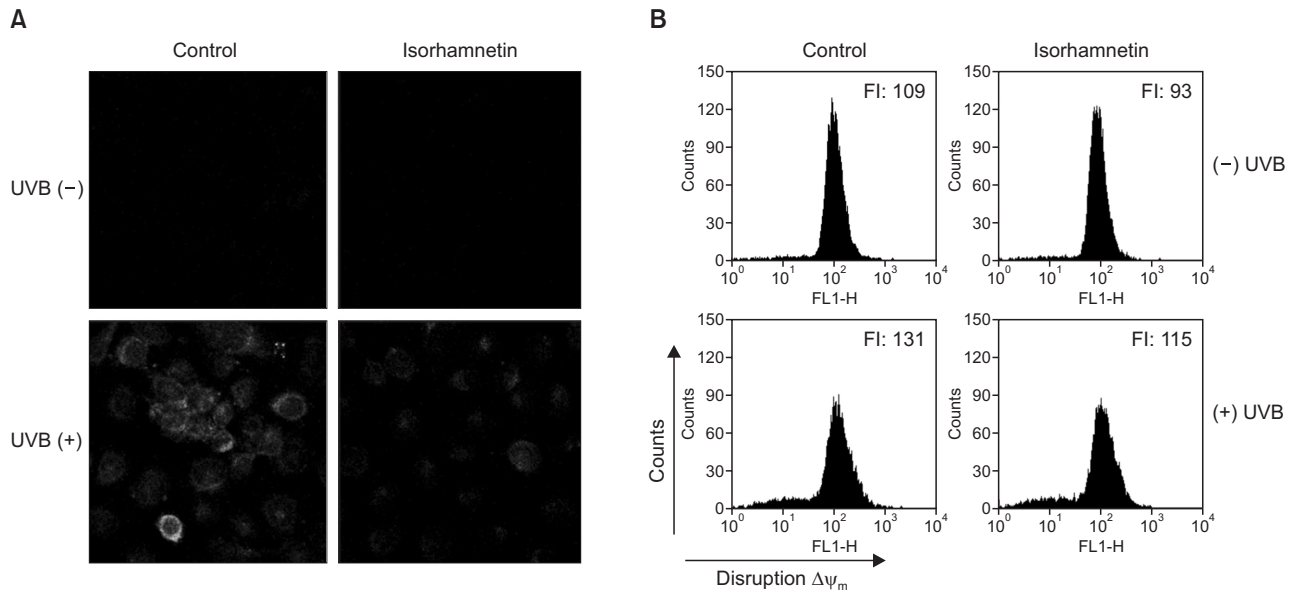

Fig. 3. Isorhamnetin inhibits UVB-induced mitochondrial dysfunction. Isorhamnetin pretreatment impedes the loss of mitochondrial membrane potential in HaCaT keratinocytes after UVB exposure, as determined by (A) confocal microscopy and (B) flow cytometry of JC-1-stained cells. FI, fluorescence intensity.

Isorhamnetin inhibits UVB-induced mitochondrial dysfunction

Apoptosis is mediated via mitochondrial membrane permeabilization/depolarization events (Landes and Martinou, 2011). Ample evidence demonstrates that UVB irradiation leads to a loss of mitochondrial membrane potential ($\Delta\psi_m$) (Kim *et al*., 2014; Mencucci *et al*., 2014). To investigate whether isorhamnetin can inhibit UVB-induced apoptosis stemming from mitochondrial dysfunction, we employed confocal microscopy and flow cytometry to measure the fluorescence intensity of JC-1 dye in HaCaT keratinocytes under various experimental conditoins. Confocal microscopy analysis showed that the mitochondria of UVB-irradiated cells strongly fluoresced green, indicative of $\Delta\psi_m$ depolarization. However, the increase in green fluorescence intensity was almost completely prevented by isorhamnetin pretreatment (Fig. 3A). These findings were confirmed by flow cytometry data (Fig. 3B), suggesting that isorhamnetin attenuates UVB-induced disruption of $\Delta\psi_m$ in HaCaT keratinocytes.

Isorhamnetin protects HaCaT keratinocytes against UVB-facilitated macromolecular damage

Excessive exposure to UVB light substantially increases DNA strand breakage in keratinocytes (de Gruijl *et al*., 2001). DNA strands breakage can be visualized and assessed by the comet assay, where DNA tail length represents the degree of DNA lesion. Both comet tail length and the percentage of total cellular fluorescence in the comet tails were clearly increased in UVB-irradiated vs. untreated control keratinocytes, whereas isorhamnetin pretreatment of UVB-exposed cells significantly decreased these values (Fig. 4A).

UVB light also causes oxidative damage to cellular lipids. Lipid peroxidation was evaluated by measurement of 8-isoprostane levels secreted into the conditioned medium of HaCaT keratinocytes. UVB-exposed cells secreted more 8-isoprostane relative to unexposed control cells, while isorhamnetin pretreatment significantly decreased 8-isoprostane content in the medium of irradiated cells, without having any effect of its own (Fig. 4B). The capability of isorhamnetin to circumvent oxidative lipid injury was confirmed by confocal microcopy of DPP oxide fluorescence in DPPP-stained cells (Fig. 4C).

Finally, protein carbonylation is an indication of oxidative stress-induced damage to macromolecular proteins (Dalle-Donne *et al*., 2003). UVB exposure significantly up-regulated protein carbonyl content in HaCaT keratinocytes, but this action was prevented by isorhamnetin pretreatment (Fig. 4D).

DISCUSSION

Isorhamnetin is a naturally occurring, methylated flavonoid. The biological activities of isorhamnetin are reportedly greater than those of its unmethylated parent compound, which might due to the increased absorption and metabolic stability of methylated flavonoids (Wen and Walle, 2006). In the current study, we investigated the antioxidant and cytoprotective effects of isorhamnetin against UVB-induced damage in keratinocytes, the predominant cell type found in the human epidermis. Our findings indicate that isorhamnetin is not cytotoxic at concentrations of ≤ 5 μM to keratinocytes (Fig. 1A), and may therefore find utility as part of a therapeutic arsenal against UVB-provoked skin damage.

Because of its special chemical structure features, the hydroxyl group is an indispensable functional group of many natural antioxidants, including isorhamnetin and other polyphenols (Sim *et al*., 2007). In general, the phenolic hydroxyl group donation of a hydrogen atom acts to effectively quench ROS (Choi *et al*., 2002; Heim *et al*., 2002; Valentão *et al*., 2003). Consistent with these reports, the present results revealed that isorhamnetin efficiently scavenged intracellular ROS in

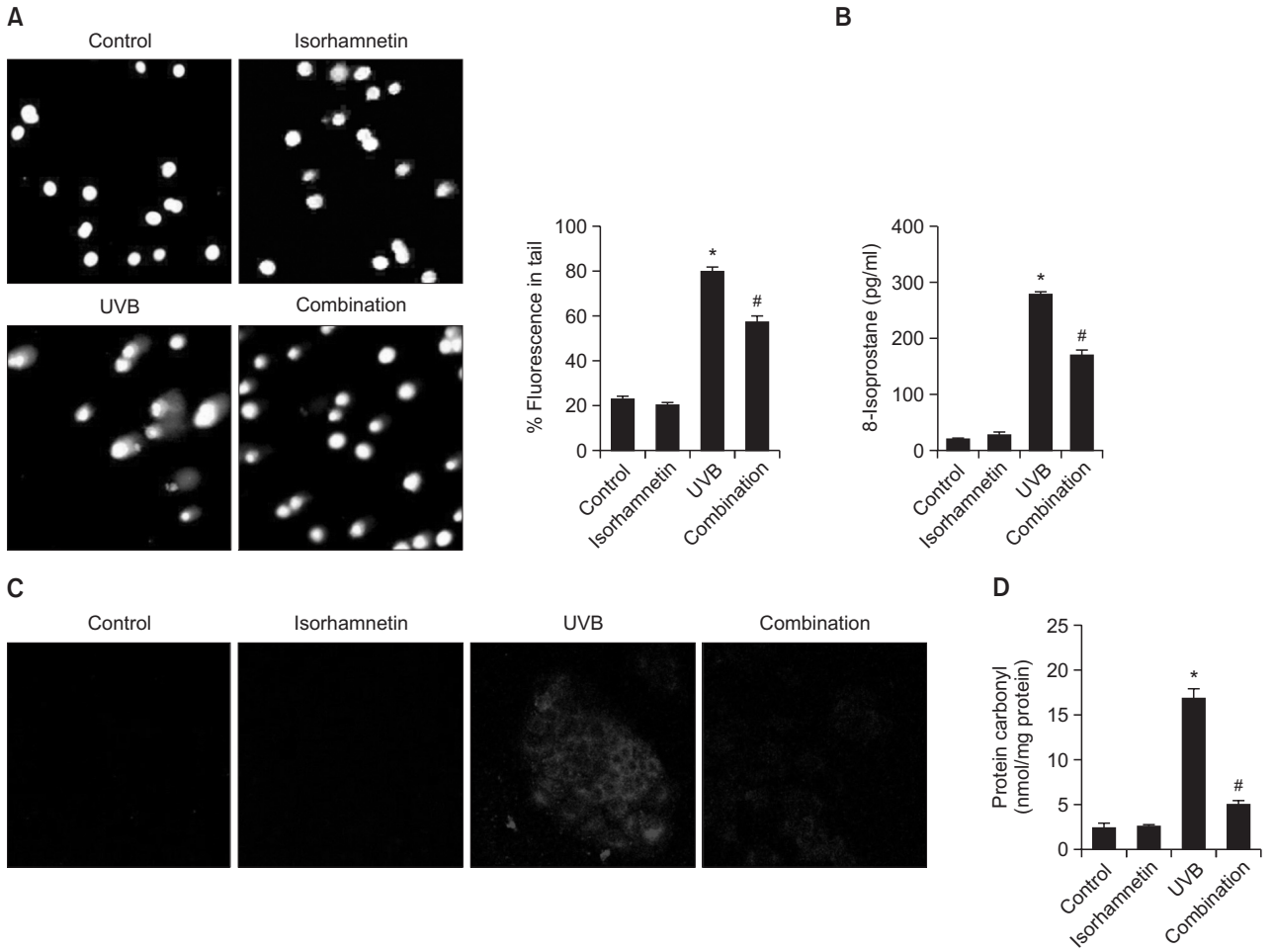

Fig. 4. Isorhamnetin protects HaCaT keratinocytes against UVB-induced oxidative macromolecular damage. (A) DNA damage was detected by the comet assay. (B and C) Lipid peroxidation was detected by (B) measurement of 8-isoprostane levels in the conditioned media and (C) detection of lipid hydroperoxides in DPPP-stained cells by fluorescence microscopy. (D) Protein oxidation was assayed by measurement of protein carbonyl levels. *Significantly different from control (p<0.05); #significantly different from UVB-irradiated cells (p<0.05). Combination, isorhamnetin+UVB light.

HaCaT keratinocytes (Fig. 1B-D), and also directly quenched the superoxide anion and the hydroxyl radical in cell-free systems (Fig. 1E, F). Therefore, the ROS scavenging ability of isorhamnetin may be due to the phenolic hydroxyl groups in its structure.

UVB-induced apoptosis is mediated by a number of molecular processes, which target the mitochondria and activate the mitochondria-initiated cell death pathway (Ji *et al*., 2015). These processes include changes in the $\Delta\psi_m$ opening of the mitochondrial permeability transition pore, and release of cytochrome c from the mitochondrion into the cytoplasm. Consequently, mitochondria rapidly lose their transmembrane potential during apoptosis, generating excessive amounts of intracellular ROS (Ricci *et al*., 2003) and attenuating cell viability. In addition to substantially protecting human keratinocytes from UVB-provoked programmed cell death and mitochondrial dysfunction (Fig. 2, 3), isorhamnetin also rescued cell viability in UVB-exposed HaCaT keratinocytes (Fig. 2).

Abnormal production of ROS leads to oxidative damage to macromolecules, including DNA, lipids, and proteins (Pashikanti *et al*., 2011; Ray *et al*., 2012). Like apoptosis and mitochondrial dysfunction, macromolecular injury contributes to considerable disruption of normal cellular functions. Notably, the present study showed that isorhamnetin pretreatment also prevented DNA strand breakage, lipid peroxidation, and protein carbonyl formation in HaCaT keratinocytes following exposure to UVB light (Fig. 4).

In conclusion, the results of this study demonstrate that isorhamnetin suppresses the deleterious effects of UVB irradiation in human keratinocytes, including excessive intracellular ROS generation, oxidative damage to DNA, lipids, and proteins, and mitochondrial dysfunction. Moreover, isorhamnetin improves cell viability and inhibits apoptosis in UVB-exposed human keratinocytes. These data support the hypothesis that isorhamnetin might be utilized as a novel antioxidant agent to treat ROS-related skin disorders. Nevertheless, the biological efficacy of isorhamnetin *in vivo* and the underlying mechanisms of isorhamnetin action require further exploration.

ACKNOWLEDGMENTS

This work was supported by the R&D Program of Plasma Advanced Technology for Agriculture and Food (Plasma Farming) through the National Fusion Research Institute of Korea (NFRI) funded by the Government.

REFERENCES

Afaq, F. (2011) Natural agents: cellular and molecular mechanisms of photoprotection. *Arch. Biochem. Biophys.* **508**, 144-151.

Beauchamp, M. C., Letendre, E. and Renier, G. (2002) Macrophage lipoprotein lipase expression is increased in patients with heterozygous familial hypercholesterolemia. *J. Lipid Res.* **43**, 215-222.

Budden, T. and Bowden, N. A. (2013) The role of altered nucleotide excision repair and UVB-induced DNA damage in melanomagenesis. *Int. J. Mol. Sci.* **14**, 1132-1151.

Carmichael, J., DeGraff, W. G., Gazdar, A. F., Minna, J. D. and Mitchell, J. B. (1987) Evaluation of a tetrazolium-based semiautomated colorimetric assay: assessment of chemosensitivity testing. *Cancer Res.* **47**, 936-946.

Choi, H. R., Choi, J. S., Han, Y. N., Bae, S. J. and Chung, H. Y. (2002) Peroxynitrite scavenging activity of herb extracts. *Phytother. Res.* **16**, 364-367.

Cossarizza, A., Baccarani-Contri, M., Kalashnikova, G. and Franceschi, C. (1993) A new method for the cytofluorimetric analysis of mitochondrial membrane potential using the J-aggregate forming lipophilic cation 5,5',6,6'-tetrachloro-1,1',3,3'-tetraethylbenzimidazolcarbocyanine iodide (JC-1). *Biochem. Biophys. Res. Commun.* **197**, 40-45.

Dalle-Donne, I., Rossi, R., Giustarini, D., Milzani, A. and Colombo, R. (2003) Protein carbonyl groups as biomarkers of oxidative stress. *Clin. Chim. Acta* **329**, 23-38.

de Gruijl, F. R., van Kranen, H. J. and Mullenders, L. H. (2001) UV-induced DNA damage, repair, mutations and oncogenic pathways in skin cancer. *J. Photochem. Photobiol. B* **63**, 19-27.

Everett, M. A., Yeargers, E., Sayre, R. M. and Olson R. L. (1966) Penetration of epidermis by ultraviolet rays. *Photochem. Photobiol.* **5**, 533-542.

Heim, K. E., Tagliaferro, A. R. and Bobilya, D. J. (2002) Flavonoid antioxidants: chemistry, metabolism and structure-activity relationships. *J. Nutr. Biochem.* **13**, 572-584.

Helenius, M., Makelainen, L. and Salminen A. (1999) Attenuation of NF-kappaB signaling response to UVB light during cellular senescence. *Exp. Cell Res.* **248**, 194-202.

Ji, Y., Cai, L., Zheng, T., Ye, H., Rong, X., Rao, J. and Lu, Y. (2015) The mechanism of UVB irradiation induced-apoptosis in cataract. *Mol. Cell. Biochem.* **401**, 87-95.

Kim, K. C., Piao, M. J., Zheng, J., Yao, C. W., Cha, J. W., Kumara, M. H., Han, X., Kang, H. K., Lee, N. H. and Hyun, J. W. (2014) Fucodiphlorethol G purified from *Ecklonia cava* suppresses ultraviolet B radiation-induced oxidative stress and cellular damage. *Biomol. Ther.* **22**, 301-307.

Kohno, M., Mizuta, Y., Kusai, M., Masumizu, T. and Makino, K. (1994) Measurements of superoxide anion radical and superoxide anion scavenging activity by electron spin resonance spectroscopy coupled with DMPO spin trapping. *Bull. Chem. Soc. Jpn.* **67**, 1085-1090.

Landes, T. and Martinou, J. C. (2011) Mitochondrial outer membrane permeabilization during apoptosis: the role of mitochondrial fission. *Biochim. Biophys. Acta* **1813**, 540-545.

Lee, C. W., Ko, H. H., Chai, C. Y., Chen, W. T., Lin, C. C. and Yen, F. L. (2013) Effect of *Artocarpus communis* extract on UVB irradiation-induced oxidative stress and inflammation in hairless mice. *Int. J. Mol. Sci.* **14**, 3860-3873.

Li, C., Yang, X., Chen, C., Cai, S. and Hu, J. (2014) Isorhamnetin suppresses colon cancer cell growth through the PI3K-Akt-mTOR pathway. *Mol. Med. Rep.* **9**, 935-940.

Li, L., Abe, Y., Kanagawa, K., Usui, N., Imai, K., Mashino, T., Mochizuki, M. and Miyata, N. (2004) Distinguishing the 5,5-dimethyl-1-pyrroline N-oxide (DMPO)-OH radical quenching effect from the hydroxyl radical scavenging effect in the ESR spin-trapping method. *Anal. Chim. Acta* **512**, 121-124.

Liu, S., Guo, C., Wu, D., Ren, Y., Sun, M. Z. and Xu, P. (2012) Protein indicators for HaCaT cell damage induced by UVB irradiation. *J. Photochem. Photobiol. B* **114**, 94-101.

Lyu, S. Y. and Park, W. B. (2012) Photoprotective potential of anthocyanins isolated from *Acanthopanax divaricatus* Var. albeofructus fruits against UV irradiation in human dermal fibroblast cells. *Biomol. Ther.* **20**, 201-206.

Matsumura, Y. and Ananthaswamy, H. N. (2004) Toxic effects of ultraviolet radiation on the skin. *Toxicol. Appl. Pharmacol.* **195**, 298-308.

Mencucci, R., Favuzza, E., Boccalini, C., Lapucci, A., Felici, R., Resta, F., Chiarugi, A. and Cavone, L. (2014) CoQ10-containing eye drops prevent UVB-induced cornea cell damage and increase cornea wound healing by preserving mitochondrial function. *Invest. Ophthalmol. Vis. Sci.* **55**, 7266-7271.

Okimoto, Y., Watanabe, A., Niki, E., Yamashita, T. and Noguchi, N. (2000) A novel fluorescent probe diphenyl-1-pyrenylphosphine to follow lipid peroxidation in cell membranes. *FEBS Lett.* **474**, 137-140.

Pashikanti, S., Boissonneault, G. A. and Cervantes-Laurean, D. (2011) Ex vivo detection of histone H1 modified with advanced glycation end products. *Free Radic. Biol. Med.* **50**, 1410-1416.

Rajagopalan, R., Ranjan, S. and Nair, C. K. (2003) Effect of vinblastine sulfate on gamma-radiation-induced DNA single-strand breaks in murine tissues. *Mutat. Res.* **536**, 15-25.

Ray, P. D., Huang, B. W. and Tsuji, Y. (2012) Reactive oxygen species (ROS) homeostasis and redox regulation in cellular signaling. *Cell. Signal.* **24**, 981-990.

Ricci, J. E, Gottlieb, R. A. and Green, D. R. (2003) Caspase-mediated loss of mitochondrial function and generation of reactive oxygen species during apoptosis. *J. Cell Biol.* **160**, 65-75.

Rosenkranz, A. R., Schmaldienst, S., Stuhlmeier, K. M., Chen, W., Knapp, W. and Zlabinger, G. J. (1992) A microplate assay for the detection of oxidative products using 2′,7′-dichlorofluorescin-diacetate. *J. Immunol. Methods* **156**, 39-45.

Rosette, C. and Karin, M. (1996) Ultraviolet light and osmotic stress: activation of the JNK cascade through multiple growth factor and cytokine receptors. *Science* **274**, 1194-1197

Sander, C. S., Chang, H., Hamm, F., Elsner, P. and Thiele, J. J. (2004) Role of oxidative stress and the antioxidant network in cutaneous carcinogenesis. *Int. J. Dermatol.* **43**, 326-335.

Scandalios, J. G. (2002) The rise of ROS. *Trends Biochem. Sci.* **27**, 483-486.

Schwarz, A., Bhardwaj, R., Aragane, Y., Mahnke, K., Riemann, H., Metze, D., Luger, T. A. and Schwarz, T. (1995) Ultraviolet-B-induced apoptosis of keratinocytes: evidence for partial involvement of tumor necrosis factor-α in the formation of sunburn cells. *J. Invest. Dermatol.* **104**, 922-927.

Sim, G. S., Lee, B. C., Cho, H. S., Lee, J. W., Kim, J. H., Lee, D. H., Kim, J. H., Pyo, H. B., Moon, D. C., Oh, K. W., Yun, Y. P. and Hong, J. T. (2007) Structure activity relationship of antioxidative property of flavonoids and inhibitory effect on matrix metalloproteinase activity in UVA-irradiated human dermal fibroblast. *Arch. Pharm. Res.* **30**, 290-298.

Singh, N. P. (2000) Microgels for estimation of DNA strand breaks, DNA protein crosslinks and apoptosis. *Mutat. Res.* **455**, 111-127.

Ueno, I., Kohno, M., Yoshihira, K. and Hirono, I. (1984) Quantitative determination of the superoxide radicals in the xanthine oxidase reaction by measurement of the electron spin resonance signal of the superoxide radical spin adduct of 5,5-dimethyl-1-pyrroline-1-oxide. *J. Pharmacobiodyn.* **7**, 563-569.

Valentão, P., Fernandes, E., Carvalho, F., Andrade, P. B., Seabra, R. M. and Bastos, M. L. (2003) Hydroxyl radical and hypochlorous acid scavenging activity of small centaury (*Centaurium erythraea*) infusion. A comparative study with green tea (*Camellia sinensis*). *Phytomedicine* **10**, 517-522.

Wäster, P. K. and Ollinger, K. M. (2009) Redox-dependent translocation of p53 to mitochondria or nucleus in human melanocytes after UVA- and UVB-induced apoptosis. *J. Invest. Dermatol.* **129**, 1769-

1781.
Wen, X. and Walle, T. (2006) Methylated flavonoids have greatly improved intestinal absorption and metabolic stability. *Drug Metab. Dispos.* **34**, 1786-1792.
Wyllie, A., Morris, R., Smith, A. and Dunlop, D. (1984) Chromatin cleavage in apoptosis: association with condensed chromatin morphology and dependence on macromolecular synthesis. *J. Pathol.* **142**, 67-77.
Yang, J. H., Shin, B. Y., Han, J. Y., Kim, M. G., Wi, J. E., Kim, Y. W., Cho, I. J., Kim, S. C., Shin, S. M. and Ki, S. H. (2014) Isorhamnetin protects against oxidative stress by activating Nrf2 and inducing the expression of its target genes. *Toxicol. Appl. Pharmacol.* **274**, 293-301.
Yin, Y., Li, W., Son, Y. O., Sun, L., Lu, J., Kim, D., Wang, X., Yao, H., Wang, L., Pratheeshkumar, P., Hitron, A. J., Luo, J., Gao, N., Shi, X. and Zhang, Z. (2013) Quercitrin protects skin from UVB-induced oxidative damage. *Toxicol. Appl. Pharmacol.* **269**, 89-99.
Zeng, J. P., Bi, B., Chen, L., Yang, P., Guo, Y., Zhou, Y. Q. and Liu, T. Y. (2014) Repeated exposure of mouse dermal fibroblasts at a subcytotoxic dose of UVB leads to premature senescence: a robust model of cellular photoaging. *J. Dermatol. Sci.* **73**, 49-56.